JACS
JOURNAL OF THE AMERICAN CHEMICAL SOCIETY
Article
pubs.acs.org/JACS

Iron Nanoparticles Catalyzing the Asymmetric Transfer Hydrogenation of Ketones

Jessica F. Sonnenberg,[†] Neil Coombs,[†] Paul A. Dube,[‡] and Robert H. Morris*,[†]

[†]Department of Chemistry, University of Toronto, 80 St. George Street, Toronto, Ontario, M5S 3H6, Canada
[‡]Brockhouse Institute for Materials Research, McMaster University, 1280 Main Street West, Hamilton, Ontario, L8S 4M1, Canada

Supporting Information

ABSTRACT: Investigation into the mechanism of transfer hydrogenation using *trans*-[Fe(NCMe)CO($PPh_2C_6H_4CH{=}NCHR{-}$)$_2$][BF_4]$_2$, where R = H (**1**) or R = Ph (**2**) (from *R,R*-dpen), has led to strong evidence that the active species in catalysis are iron(0) nanoparticles (Fe NPs) functionalized with achiral (with **1**) and chiral (with **2**) PNNP-type tetradentate ligands. Support for this proposition is given in terms of *in operando* techniques such as a kinetic investigation of the induction period during catalysis as well as poisoning experiments using substoichiometric amounts of various poisoning agents. Further support for the presence of Fe(0) NPs includes STEM microscopy imaging with EDX analysis, XPS analysis, and SQUID magnetometry analysis of catalytic solutions. Further evidence of Fe NPs acting as the active catalyst is given in terms of a polymer-supported substrate experiment whereby the NPs are too large to permeate the pores of a functionalized polymer. Final support is given in terms of a combined poisoning/STEM/EDX experiment whereby the poisoning agent is shown to be bound to the Fe NPs. This paper provides evidence of a rare example of asymmetric catalysis with nonprecious metal, zerovalent nanoparticles.

INTRODUCTION

The synthesis of enantiopure alcohols is of vital importance in the pharmaceutical, fragrance, and food flavouring industries.[1−3] These alcohols are commonly made in industry via the selective hydrogenation of carbonyl groups by direct H_2-hydrogenation or transfer hydrogenation (TH)[4] using isopropanol as the hydrogen source. Catalysts used for these types of conversions are typically based on precious metals such as iridium, rhodium, and ruthenium.[5−7] It has therefore become very attractive to replace these precious metals with iron,[8−11] as it is significantly cheaper, more abundant, and less toxic.[12] Exploration of iron catalysts for the hydrogenation of ketones first began with work by Vancheesan et al.[13,14] whose catalytic systems were small iron carbonyl cluster compounds. Gao et al.[15] found that adding a tetradentate ligand (*S,S*)-$PPh_2C_6H_4CH_2NHC_6H_{10}NHCH_2C_6H_4PPh_2$ to the iron(0) carbonyl cluster [NEt_3H][$Fe_3H(CO)_{11}$] resulted in a system for the asymmetric transfer hydrogenation of ketones. Our group then coordinated related PNNP systems onto iron to explore both their H_2 hydrogenation and TH capabilities.[16,17] The systems were of the type *trans*-[Fe(NCMe)CO(PNNP)]-[BF_4]$_2$ as depicted in Scheme 1. These systems were found to be quite active, and further modifications to the PNNP ligand were explored, which yielded a highly active and enantioselective TH system.[18−20]

Previous studies using precatalysts **1** and **2**[21] showed an induction period during catalysis, followed by a rapid increase in rate, and eventual equilibration. Sigmoidal curves such as these are often seen in heterogeneous systems, where an active catalyst must first form[22,23] before any measurable activity is seen. Given the strongly reducing conditions for catalysis, the resultant dark color during catalysis, and our kinetic observations, we asked the question, 'Could the active species be a heterogeneous catalyst?'. The Fischer−Tropsch process[24,25] and the Haber−Bosch synthesis[26] are the two most common examples of the use of iron in heterogeneous catalysis; however a limited number of other examples do exist as olefin hydrogenation catalysts.[27−29] Iron nanoparticles are also catalysts for the formation of carbon nanotubes,[30−34] the reduction of peroxides[35] and CO_2,[36] and the hydrolytic dehydrogenation of ammonia boranes.[37] Iron oxides have been used as nanoparticle supports for heterogeneous catalysis

Scheme 1. Typical Reaction Scheme for TH, and the Precatalyst Structures

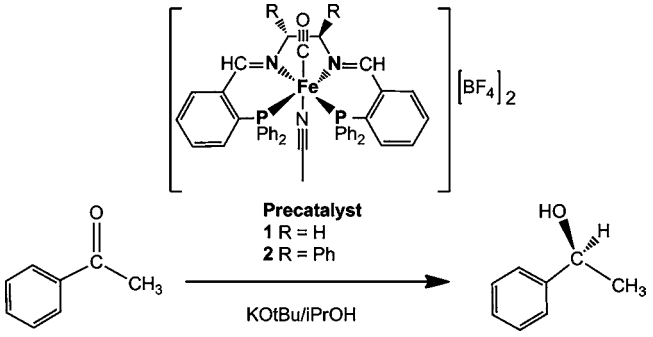

Received: December 14, 2011
Published: March 26, 2012

   dx.doi.org/10.1021/ja211658t | *J. Am. Chem. Soc.* 2012, 134, 5893−5899

with other metals as the active sites,[38−40] but the use of zerovalent iron as an active site for asymmetric catalysis has not been reported.

We recently reported an extensive spectroscopic and DFT study of the species observed during TH using **1** as the precatalyst.[41] Upon reaction of **1** with 2 equiv of sodium isopropoxide in benzene, an unusual folded ferraziridine complex $[Fe(CO)(PPh_2C_6H_4CH{=}NCH_2CH_2NHCHC_6H_4PPh_2)$-$\kappa^5P,N,C,N,P][BF_4]$ could be isolated but was found to not be catalytically active. Upon reaction of the ferraziridine complex with potassium *tert*-butoxide in isopropanol, a deprotonated ferraziridinido complex $Fe(CO)(PPh_2C_6H_4CH{=}NCH_2CH_2$-$NCHC_6H_4PPh_2)$-$\kappa^5P,N,C,N,P$ (**3**) could be observed. **3** matched the species observed by $^{31}P\{^1H\}$ NMR during TH but was also found to not be catalytically active. DFT calculations showed that formation of **3** was highly energetically favorable, as was further reduction to the Fe(0), square pyramidal species $Fe(CO)(PPh_2C_6H_4CH{=}NCH_2{-})_2$-$\kappa^4P,N,N,P$. This favorable reduction to an Fe(0) species provided support for the potential formation of Fe(0) NPs in solution during catalysis.

Nanoparticles (NPs) have been studied extensively in the past decades as possible catalysts for a variety of reactions due to the fact that they have much higher surface areas than bulk heterogeneous catalysts and can therefore be as reactive and reproducible[42] as homogeneous catalysts, but with the benefit that they are often recyclable and separable.[43] Nanoparticles are often difficult to detect as they appear homogeneous in solution,[22,23] but there are several reports of transition metal nanoparticles being well characterized and used for catalysis.[42,44−47] Iron magnetite nanoparticles have been used as supports for precious metal asymmetric catalysis,[48,49] which are often convenient in that they are magnetically separable.[50] Palladium(0) nanoparticles with a diameter of 4 nm have been modified with chiral ligands to perform asymmetric alkylations,[51] demonstrating that an enantioselective reaction is possible using colloidal metal catalysts.[43] Nickel(0) nanoparticles have also been used for the transfer hydrogenation of ketones in isopropanol,[52] demonstrating the use of nonprecious metal NP catalysts for TH. Herein we provide evidence for the first example of asymmetric catalysis using colloidal iron(0), with no precious metals present for the TH of ketones.

RESULTS AND DISCUSSION

The most common method for determining whether a catalyst is heterogeneous is the mercury poisoning test; however it has been previously reported by our group[16] that addition of Hg(0) has no effect on catalysis. This is likely due to the fact that iron does not form a stable amalgam with mercury.[53] Other well-known methods for determining whether a catalyst is heterogeneous include filtration, small molecule poisoning experiments, electron microscopy imaging, magnetometry, and X-ray photoelectron spectroscopy (XPS).[22,23,28,45,54] The most valuable of these experiments are those done *in operando*,[55] that is, while the experiment is in progress, such as kinetic and poisoning experiments, as well as multiphase experiments, which probe the catalyst while it is 'in action'. Filtration of the catalytic mixture revealed no precipitate, allowing bulk metal to be ruled out as a possible active catalyst, leaving iron(0) nanoparticles (Fe NPs) as the probable active species.

Reaction Profile. Preliminary experiments to determine the true nature of the active catalyst involved studying the kinetics of the reaction and the resultant reaction profile for TH of acetophenone to 1-phenylethanol. Both catalytic systems **1** and **2** showed a sigmoidal curve, with an induction period of 6−8 min followed by rapid catalytic activity, and a leveling off of the curve once the reaction reached equilibrium, as depicted in Figure 1. Throughout catalysis with **2**, an enantiomeric excess (ee) of approximately 64% is achieved in the product, and unlike other iron-based catalysts developed in our group,[18,56] it is only minimally diminished due to racemization with prolonged exposure to the reaction medium. This shape of curve is often indicative of heterogeneous catalysis involving colloid formation,[22,23] or autocatalysis, where the product alcohol is involved in catalysis, and therefore catalysis is slow before enough product is formed. To disprove that the system is autocatalytic due to the influence of the product alcohol, 0.2 equiv of phenylethanol (relative to acetophenone) was added to the catalytic mixture with the acetophenone during catalysis with **1** and **2**. 0.2 equiv was used because conversion to product alcohol after 10 min (after the induction period) is typically 18−20%. The conversion curves exhibited the same sigmoidal shape and the same induction period; however catalysis slowed down and equilibrium is reached sooner, due to Le Châtelier's Principle. To further probe the cause of the induction period, reactions were done where precatalyst **1** or **2** were reacted with potassium *tert*-butoxide in isopropanol for 10 min prior to the addition of substrate. Reaction curves with **1** showed no induction period, indicating that the reaction of the iron precatalyst with base to form an active species is responsible for the induction period, not the uptake of substrate. Reaction curves with (**2**) showed an increase in initial rates and a decrease in the induction period, also indicating that reduction of the iron species is necessary before the catalyst can become active. What was also interesting was the subtle increase in the enantioselectivity from 64% to 70% when the catalyst was allowed to preactivate before substrate addition. This is possibly due to the unencumbered, complete formation of the ligand-coated nanoparticles without the interference of substrate, allowing for a more optimized coating of the chiral ligand on the surface.

Poisoning Experiments. It is well reported that the use of substoichiometric amounts of small phosphines and sulphides such as PPh_3 and CS_2 as poisoning agents for catalysis is strong evidence for the formation of NPs.[22,23,28,45,54,57] Varying amounts of PMe_3 in toluene, PPh_3 in benzene, PCy_3 in toluene, $P(OMe)_3$ in benzene, $P(OPh)_3$ in toluene, $PPhMe_2$ in toluene, 1,4-diazabicyclo[2.2.2]octane (DABCO) in isopropanol, ethylene diamine in isopropanol, pentanethiol in pentane, and 2-(dimethylamino)ethanethiol in isopropanol were tested as potential poisoning agents for catalysis with both **1** and **2**. Test reactions were run by adding toluene, benzene, or pentane to the reaction mixture, to ensure no negative mixed solvent effects were observed. Amine additives, such as DABCO and ethylene diamine, had no effect on catalysis, suggesting that nitrogen donors are not suitable poisoning agents. PMe_3, when introduced as catalysis was started, prevented all conversion of ketone to alcohol. It was then added to an active catalytic mixture after the induction period in varying concentrations. Percentages of PMe_3 of 50, 20, and 10% relative to precatalyst **1** or **2** were able to completely stop conversion of ketone to alcohol, as shown in Figure 1, whereas 5 and 7% only slowed down catalysis. A minimum of 10% PMe_3 is required to stop catalysis, suggesting not only that the active species are NPs but also that 10% of the total iron is present as active sites on the surface of the NP. Alternatively, this could indicate that, if the active catalyst is homogeneous, only 10% of the iron (relative to the starting iron) is active. To disprove potential coordination of PMe_3 to the precatalyst, which would also prevent catalysis, a large excess of PMe_3 was reacted with **1** in isopropanol and

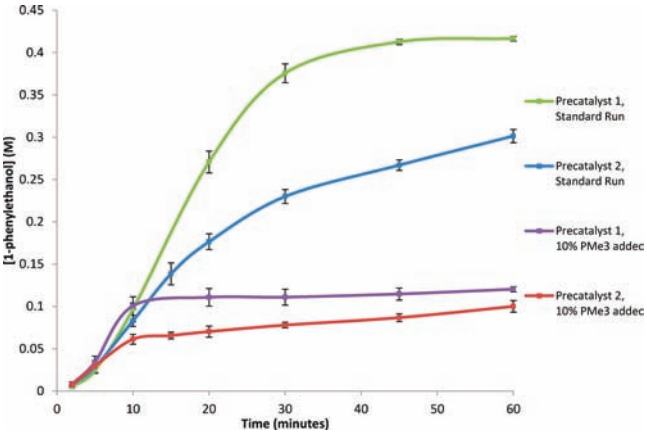

Figure 1. Standard catalytic runs using **1** and **2**, and poisoning runs using **1** and **2** and 10% PMe_3 added at t = 10 min.

studied by NMR. The $^{31}P\{^1H\}$ spectrum showed a large, broad peak for PMe_3 and a sharp, small peak for **1** as well as no peaks for the coordinated product.

To expand the range of possible phosphine poisons, various electronically and sterically different poisons were tested. 20% $P(OMe)_3$ was able to completely stop catalysis with **1**, and drastically slowed down catalysis with **2**, suggesting a minimal effect of changing the electronics of the poisoning agent, possibly due to the fact that both are able to bind strongly enough to iron. PPh_3 and PCy_3 were also tested as potential poisoning agents. To our surprise, when 20% PCy_3 was added to active catalytic mixtures of **1** or **2**, conversion rates increased and the overall ee was unaffected for catalysis with **2**. The addition of PPh_3 appeared to have no effect on catalysis with **1** but increased conversion rates slightly with **2**. These results suggest a strong dependence on the steric bulk of the phosphine used and that poisoning effects could be explained based on Tolman cone angles.[58] To further study the effects of the sterics of the poisoning agent, $PPhMe_2$ was tested, which is slightly bulkier than the effective PMe_3. Similarly to PMe_3, catalysis was completely stopped with both **1** and **2**, indicating that sterics does play a significant role in the phosphines' poisoning ability. We are still investigating why the conversion rates increase when bulky phosphine groups are added; they may space themselves out near the surface leaving access to catalytically active sites, unlike PMe_3, yet preventing agglomeration of the NPs. This phenomenon is difficult to explain from a homogeneous catalyst point of view; the displacement of part of the PNNP ligand by PCy_3 may be feasible but would likely change the enantioselectivity of the reaction. Small phosphines such as PMe_3 may be able to penetrate into the NP shell and bind directly to the Fe active sites, preventing catalysis.

The last type of poisoning agent we were interested in studying the effects of were sulfur donors, as it is well reported that carbon disulfide[22,57] is a well-known poison for heterogeneous catalysts. The thiol, 2-(dimethylamino)ethanethiol, at 20% relative to iron, drastically slowed down catalysis with **1** and partially slowed down catalysis with **2**, suggesting that the active species is sensitive to sulfur-containing compounds. Pentanethiol, at 15% relative to iron, was also tested, as it is slightly less bulky than 2-(dimethylamino)ethanethiol, and sterics had already proven to be very important in terms of poisoning effects. 15% pentanethiol was as effective as PMe_3 at poisoning (**2**), showing that the subtle steric change was effective. Interestingly, when 15% pentanethiol was used as a poison with **1**, the rate decreased considerably; however catalysis was not as completely poisoned as it was with PMe_3, but rather was very similar to poisoning with 2-(dimethylamino)ethanethiol. Poisoning experiments therefore demonstrate that the ethylenediamine and *R,R*-diphenyl-ethylenediamine backbones of **1** and **2** play a significant role in catalysis, which results in differences in the poisoning behavior for catalysis with **1** and **2**. Catalysis with **2** seems to be more sensitive to steric changes in the poisoning agents, likely because its backbone is much bulkier,[58] whereas **1** is poisoned more completely by a wide range of reagents and shows less extreme steric sensitivity compared to that witnessed with **2**.

XPS. X-ray Photoelectron Spectroscopy (XPS) was run on a catalytically active sample with **1** and sodium isopropoxide as the base. Solutions were dried on a sample grid and briefly exposed to air before analysis. Initial survey scans allowed for the identification of all elements present, which was followed by high resolution scans on the P 2p, N 1s, O 1s, Fe 2p, Ag 3d, and C 1s, all of which are outlined in further detail in the Supporting Information. Phosphorus was present in two different bonding states, likely caused by phosphorus present in both tri- and pentavalent states. $^{31}P\{^1H\}$ NMR studies during catalysis with **1** show that both a free ligand (trivalent P) and an oxidized free ligand (pentavalent P) are present,[41] which could account for two binding states present in the XPS spectrum. Iron was found to be present in three bonding states, the largest of which corresponds to Fe(0), and the remaining two corresponding to Fe_2O_3 and a shakeup satellite peak.[59,60] During analysis, since the sample is exposed briefly to air, the formation of surface iron oxides is inevitable, resulting in the peaks seen in the XPS.

STEM. Scanning Transmission Electron Microscopy (STEM) imaging was carried out on catalytically active samples of **1** and of **2** with sodium isopropoxide as the base, acetone as the substrate, and isopropanol as the TH solvent. Sodium isopropoxide was chosen as the base because the sodium cations formed crystals with tetrafluororoborate anions which were more easily distinguished than potassium from the iron samples during analysis. Acetone was used as the reacting ketone due to its low boiling point and rapid evaporation from the EM grids before analysis. Imaging of both samples revealed clusters of varying sizes, identified as agglomerated iron nanoparticles. Agglomeration is possibly caused by drying effects on the EM grids before analysis, or the presence of agglomerated species in solution caused by catalyst degradation. The NPs were measured to be 4.5 $\pm$ 1.2 nm in diameter, similar to those previously reported.[27] Typical images for solutions from catalysis with **1** and **2** are shown in Figure 2.

To confirm that the nanoparticle clusters were in fact Fe NPs, Energy-Dispersive X-ray Spectroscopy (EDX) linescans were collected on several clusters formed from both **1** and **2**. Individual linescan profiles for titanium, iron, carbon, oxygen, phosphorus, and nitrogen were acquired and analyzed. Titanium was used as a background marker and showed minimal signal, which was used to determine the amount of background in the other profiles. Iron scans showed an intense Fe signal through the sample clusters with negligible amounts of iron present on the adjacent carbon support film. This indicates that the clusters are in fact iron NPs, and there is a negligible amount of homogeneously dispersed iron in the remaining solution. Carbon signals were strong throughout due to the fact that copper grids coated with a carbon were used for analysis. Nitrogen and phosphorus both showed significantly weaker

dx.doi.org/10.1021/ja211658t | J. Am. Chem. Soc. 2012, 134, 5893−5899

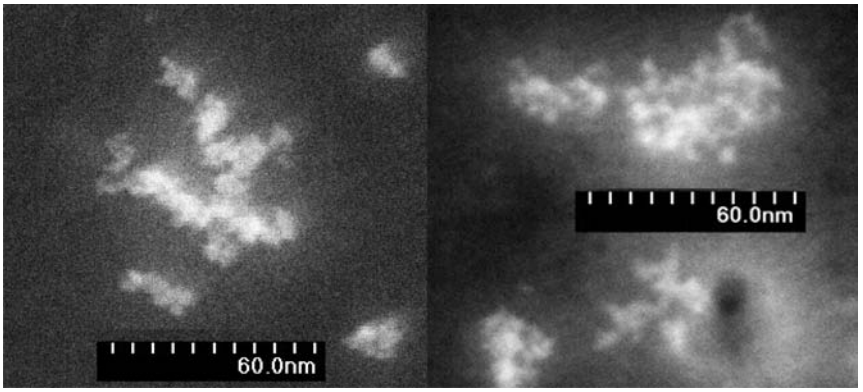

Figure 2. STEM images of TH with **1** (left) and **2** (right).

signals through the cluster, consistent with a solid iron core and a ligand functionalized shell. Nitrogen and phosphorus were also present outside of the clusters, indicating that there is some ligand in solution, unbound to the Fe NPs. This was also seen in NMR spectra of TH experiments. Free ligand and various isomers of free ligand were seen in the ^{31}P $\{^{1}H\}$ NMR of the TH solution, along with the oxidized free ligand.[41] Oxygen showed a relatively strong signal through the clusters, likely due to some surface CO, residual alkoxides, and inevitable surface oxidation forming Fe_2O_3 due to exposure to air prior to analysis.

SQUID. Superconducting Quantum Interference Device (SQUID) Magnetometry was used to determine the magnetic properties of TH solutions formed using both **1** and **2**. TH solutions were concentrated under reduced pressure to 0.15 mL in standard NMR tubes and flame-sealed under vacuum to prepare samples. Two sets of experiments were run on each sample. The first is a zero field cool-field cool (ZFC-FC) experiment, where samples were cooled in zero field to 2 K, warmed gradually under the influence of a magnetic field to 100 K, and then cooled back to 2 K under the same field. **1** and **2** show a deviation between the plots of the ZFC versus the FC experiments, indicating that the samples are not paramagnetic. Paramagnetic samples, or samples with paramagnetic impurities, do not show this type of behavior.[61] Both ZFC plots show an increase in signal with increasing temperature up to the blocking temperature of 6 K (**1**) and 7 K (**2**), where the signal reaches a maximum. This behavior is consistent with superparamagnetic particles, which is to be expected for Fe NPs, as was seen for similarly sized FeNPs previously reported.[28] Blank samples containing solely isopropanol and small amounts of potassium *tert*-butoxide showed a weak diamagnetic response. In the ZFC-FC run for **2**, the plot drops to a negative (diamagnetic) signal beyond 38 K, due to a more dilute sample (in iron) and solvent dominating the overall signal.

The second experiment involves raising and lowering the magnetic field under a constant, set temperature and analyzing the resultant hysteresis loops. **1** shows a coercive field of 400 Oe at 2 K, 175 Oe at 10 K, and 0 Oe at 50 K. This is again consistent with superparamagnetic behavior.[28,61] This change from the 'blocked' regime to the superparamagnetic regime is governed by temperature, particle size, and composition. The species generated from **2**, similar to the species generated from **1**, shows no coercive field at higher temperatures but a coercive field of 32 Oe at 2 K. The lower value can likely be attributed to a lower concentration of iron in the sample and a different composition of the nanoparticles due to the varied ligand.

Polymer-Bound Substrate Experiments. '*Ex situ*' techniques such as STEM and SQUID, along with XPS, confirmed the presence of Fe(0) NPs in the catalytic reaction mixture, but these techniques alone do not provide proof that the NPs are the catalytically active species. Kinetic and poisoning experiments are powerful *in operando* techniques that provide strong evidence of this, but they cannot completely rule out trace amounts of a homogeneous species as the active catalyst. For this, we first turned to porous polymer supported substrates and, using a similar technique employed by Witham,[62] tested the relative size of our catalysts compared to known reductants. Using a commercially available Wang resin, pyridinium chlorochromate (PCC) was used to selectively oxidize the −OH functionality to form a benzaldehyde-like substrate within the pores of the polymer. The polymer was then reacted with (**2**) and other well-known reductants, such as the Meerwein−Pondorf−Verley catalyst $AlMe_3$[63] and sodium borohydride, to reduce the C═O back to C—OH. Complex **2** provides an active catalyst for the reduction of free benzaldehyde, as has been previously reported.[16] The polymers were analyzed by infrared spectroscopy; however the —OH region was strongly affected by solvents used, and therefore modifications to the polymer were necessary to gauge the extent of conversion back to —OH. Acetic anhydride was reacted with the resultant polymer, to selectively react with the —OH and not the C═O, yielding an easily distinguished O—C═O peak in the IR. These reactions are summarized in Scheme 2. Unfortunately, isopropanol is an inadequate swelling solvent for Wang resins,[64] and therefore a 1:1 solvent mixture of tetrahydrofuran and isopropanol was necessary for the TH reaction with **2** and the $NaBH_4$ reduction. Toluene is an adequate swelling solvent for the Wang resin, and therefore no modifications were needed for catalysis with $AlMe_3$ from the previously reported method. [Note: Relative swelling of Wang resin in isopropanol/toluene/tetrahydrofuran = 1:2:3.[64]]

$NaBH_4$ was able to completely reduce the benzaldehyde-modified resin, determined by the disappearance of the C═O (benzaldehyde) peak at 1685 cm^{-1} in the IR, as well as a drastic increase in the —OH peak at 3436 cm^{-1}. This was confirmed by the appearance of an O—C═O peak at 1740 cm^{-1} upon reaction with acetic anhydride. Even at very high catalyst-to-substrate loadings (1:50, typical catalysis is with 1:600), **2** was not able to reduce the aldehyde to alcohol, determined by no disappearance of the C═O (benzaldehyde) peak, as well as negligible appearance of the O—C═O peak at 1750 cm^{-1} for an acetic anhydride reacted alcohol. Further experiments showed that three sequential additions of catalyst over 9 h

Scheme 2. Polymer-Bound Substrate Experimental Overview

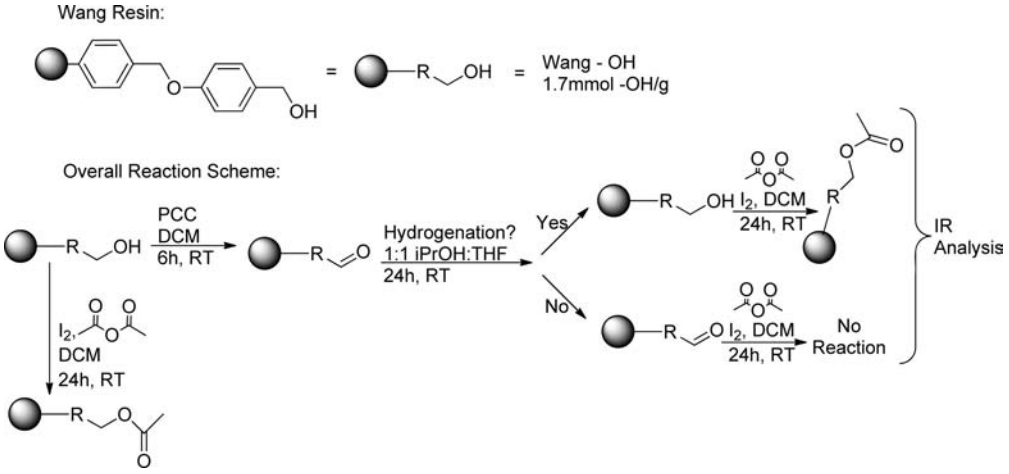

(12 mg; 0.0114 mmol each for ~0.6 mmol of C═O) yielded the same negative result as a single addition of catalyst, strongly suggesting that the catalyst is unable to get within the pores of the polymer beads. $AlMe_3$ has been previously reported to catalyze the TH of benzaldehyde to benzyl alcohol at fairly high catalyst loadings of 1:10 (catalyst/substrate).[63] Similarly to catalysis with **2**, three sequential additions of $AlMe_3$ (0.042 mmol each for ~0.42 mmol of C═O) over 9 h were used. IR showed a significant decrease of the C═O (benzaldehyde) peak, and reaction with acetic anhydride showed the appearance of an O—C═O peak at 1738 cm^{-1}, proving that the catalyst was able to get into the pores and reduce the aldehyde. These results are significant as they prove that well-known homogeneous catalysts and reagents are able to get into the pores, while the nanoparticles derived from **2** are too large and are not able to enter.

To ensure that the PCC reaction is high yielding, the benzaldehyde-modified resin was reacted with acetic anhydride, and IR showed negligible appearance of the O—C═O peak. To ensure that the acetic anhydride reaction is high yielding, the acetic anhydride modified resin was reacted with PCC, and IR showed negligible appearance of the C═O (benzaldehyde) peak. It is well reported that $NaBH_4$ is able to reduce benzaldehyde,[65] and $AlMe_3$ is also reported to effectively reduce benzaldehyde to benzyl alcohol at 90% yield in 2 h with a substrate-to-catalyst loading of 10:1. **2** was tested as a catalyst for the hydrogenation of benzaldehyde under standard TH conditions using potassium *tert*-butoxide in isopropanol and yielded 55% conversion in 1 h with a substrate-to-catalyst loading of 430:1.

STEM/EDX/Poisoning Experiments. In order to confirm that the active species during TH are Fe NPs, we combined poisoning experiments with STEM/EDX techniques to 'capture' the active species. 10% PMe_3 and 15% $CH_3(CH_2)_4SH$ relative to **2** both completely poison catalysis, indicating that the 'P' of PMe_3 and 'S' of $CH_3(CH_2)_4SH$ bind to the active sites of the catalyst, blocking the substrate from being hydrogenated. Therefore, the active species will show an increase in the amount of 'P' or 'S' relative to Fe after a sample has been poisoned. To visually analyze and quantify this we analyzed two separate STEM grids; one grid was coated with a standard TH solution (**A**), prepared as described above, and the second (**B**) was coated with a poisoned TH solution. **B** was prepared by poisoning solution **A** at t = 15 min with 15% $CH_3(CH_2)_4SH$ and then allowing the poison to bind to the active species for 10 min before preparing the grid for analysis. Agglomerated clusters (24) on each grid were analyzed using EDX to determine relative weight % of Fe/S, and the results are summarized in Table 1.

Table 1. Relative Weight Percent of Fe:S on Grids A and B Determined Using EDX at −100 °C on an STEM[a]

Standard			Add 15% S		
	Weight% Fe	Weight% S		Weight% Fe	Weight% S
Average	94.4	5.6	Average	86.1	13.9
Std. Dev.	3.3	3.3	Std. Dev.	5.2	5.2
Variance	10.6	10.6	Variance	26.7	26.7

[a]Note: Average, Standard Deviation and Variance have been calculated based on 23 values; one outlier from each series has been omitted.

In order to determine whether the results are statistically relevant, we calculated the Student's t-value for two samples with unequal variances to yield t = 6.525. This value of 't' indicates that the average weight % S on the two grids is statistically different at the 99.95% confidence interval, calculated based on 39 degrees of freedom (t_{40} = 3.551 at 99.95% C.I.) . Overall, this experiment demonstrates that when 15% pentanethiol is added to an active TH solution, the sulfur binds to the Fe NPs and stops catalysis, strongly suggesting that the iron nanoparticles are the active species in solution. The molar ratio of sulfur to iron that is calculated from the weight percent values of Table 1 is approximately 0.22:1.0 or 0.13:1.0 if the background signal is subtracted. A 4 nm iron particle has about half of the iron on the surface (as calculated in the Supporting Information), not all of which will form active sites. Thus this ratio is reasonable. It is also supported by similar values seen for other poisoned NPs in the literature such as 0.12 for Rh(0) NPs,[55] 0.2 PPh_3 for $Ir_{\sim 300}$ clusters,[42] and many more.[22,23,45,57]

$CH_3(CH_2)_4SH$ was chosen for this experiment series instead of PMe_3 because the standard TH solutions do not contain sulfur, but there is a fairly strong phosphorus signal in the background due to the PNNP ligand present. This background created too much error for the results to be statistically relevant.

Description of FeNPs. We hypothesize that upon reaction with base the Fe-PNNP complex loses its acetonitrile ligand and is reduced to an Fe(0) species, which, according to previous DFT studies, is energetically favorable.[41] Some PNNP

dx.doi.org/10.1021/ja211658t | J. Am. Chem. Soc. 2012, 134, 5893−5899

ligand then dissociates, as seen in the STEM EDX linescans and ^{31}P $\{^{1}H\}$ NMR, and the Fe(0)−CO NPs then form. Enantioselectivity is thought to be caused by the chiral PNNP-dpen backbone, which likely coordinates onto the surface of the formed NP, similar to the binding of cinchonidine on zerovalent platinum nanoparticles.[50,66] Selective binding of the PNNP ligand would thus affect the environment of the active center for catalysis, yielding alcohols with reasonably high ee (65% for acetophenone). The exact mechanism responsible for the unprecedented high ee is still under investigation; however we postulate that the surface of the NP must be very regular for the ligands to bind in such a way as to produce such high enantioselectivities. A thorough DFT and STEM study was recently published[67] outlining the specific binding of chiral modifiers to a platinum surface whereby the ligands and activated acetophenone substrate were shown to have preferred binding sites on the surface, giving further support that asymmetric catalysis is feasible on an NP surface.

One possible explanation for this regularity is outlined by Wang,[68] who discovered that, at room temperature, Fe NPs favor a cubic structure, whereby most of the particles are confined only to the six {100} planes, and not truncated by the {110} planes. This would force most of the Fe atoms to be in regular intervals and all active sites along the 'faces of the cubes' to be identical, leaving only a small fraction of the atoms along the edges of the cubes to negatively affect the regularity. This phenomenon was primarily seen for Fe(0) NPs coated in iron oxide, giving a total diameter of >8 nm, which is larger than the particles we report; however this favorability toward the cubic Fe bcc structure may still dominate in the case of our catalysis.

Several attempts have been made to synthesize Fe(0) NPs independently using well reported techniques and functionalize them with our PNNP ligands. Bedford,[69] Phua,[27] and Rangheard[28] have described syntheses and characterizations of Fe(0) NPs formed by the reduction of iron(II) and iron(III) halides using aryl and alkyl Grignard reagents, often in the presence of stabilizing reagents such as polyethylene glycol (PEG). We tested NPs formed using this method for the TH of ketones and found that they were not active, nor were NPs formed using several variations of this method in the presence of PNNP ligands or PNNP-ligand precursors as a template technique. This remained the case whether the ligand was added during synthesis or to the preformed NPs, and whether synthesis was carried out under an atmosphere of CO or not. Other reported methods for the synthesis of well-defined Fe(0) NPs involve the carbothermal reduction of iron salts on carbon black, as reported by Hoch.[70] These NPs were not catalytically active for the TH of ketones or upon reaction with PNNP ligand. Attempts were also made to immobilize iron salts onto carbon and reduce using Grignard reagents to make carbon supported Fe(0) NPs of a smaller diameter than those reported by Hoch. These were treated with PNNP ligands, either during or after synthesis, and both with and without CO present; however no catalytic activity for the TH of ketones was observed. Iron(0) powders described by Kavaliunas[71] were also synthesized and tested for catalysis with PNNP ligands; however these were also found to be inactive. All of these attempts to synthesize Fe(0) NPs using different methods did not yield active catalysts, thus showing that a very intricate balance of starting materials and conditions are required to form the NPs formed during our catalysis.

CONCLUSIONS

Upon investigating the mechanism of asymmetric transfer hydrogenation of ketones with our *trans*-[Fe(NCMe)CO-$(PPh_2C_6H_4CH{=}NCHR{-})_2$][BF_4]$_2$ (R = H, Ph) precatalyst we discovered by STEM, SQUID, and XPS analyses that Fe(0) NPs were being formed during catalysis. STEM showed that the NPs are approximately 4.5 nm in diameter, SQUID showed that the catalytic mixture contained primarily a superparamagnetic species, and XPS analysis confirmed the formation of an Fe(0) species. Kinetic analysis confirmed that activation of the Fe precatalyst with base and isopropanol was responsible for the induction period, resulting in a sigmoidally shaped reaction profile. Several poisoning agents were tested, and PMe_3 proved the most effective, completely stopping catalysis with only a 10% loading of poison relative to the catalyst. Functionalization of a porous Wang resin with a benzaldehyde-like functionality and subsequent reaction with various hydrogenation catalysts and reagents proved that well-defined homogeneous species were able to get within the pores but that the catalyst derived from **2** is too large, thereby providing further evidence that the active species are NPs. Pentanethiol was shown to be an effective substoichiometric poisoning agent, and using STEM/EDX techniques it was demonstrated to bind to the Fe NPs, providing strong evidence that NPs are the active species in catalysis.

It is very difficult to rule out completely the operation of a small amount of homogeneous catalyst generated in the mixture during the activation process. Related iron catalyst systems appear to operate by a homogeneous mechanism.[18,20]

This is, to the best of our knowledge, a rare example of highly active asymmetric catalysis using zerovalent nanoparticles not based on precious metals.[72] This also suggests that asymmetric induction is not adequate proof of homogeneous over heterogeneous catalysis.

ASSOCIATED CONTENT

Supporting Information

Experimental procedures, NMR spectra, plots of all catalytic runs and poisoning experiments, XPS spectra and data, STEM imaging and EDX linescan plots, SQUID plots, polymer-bound substrate experiment results, complete Poisoning/EDX experimental results, and more details on various attempts to form Fe(0) NPs using alternative methods are available. This material is available free of charge via the Internet at http://pubs.acs.org.

AUTHOR INFORMATION

Corresponding Author

rmorris@chem.utoronto.ca

Notes

The authors declare no competing financial interest.

ACKNOWLEDGMENTS

We thank NSERC for a Discovery grant to R.H.M. and graduate scholarships for J.F.S. We would like to thank Dr. Rana Sodhi, Dr. Darcy Burns, and Dr. Ilya Gourevich for their invaluable help and expertise in analysis by XPS, NMR, and microscope imaging, respectively.

REFERENCES

(1) Blaser, H. U.; Malan, C.; Pugin, B.; Spindler, F.; Steiner, H.; Studer, M. *Adv. Synth. Catal.* **2003**, *345*, 103−151.

(2) Naud, F.; Spindler, F.; Rueggeberg, C. J.; Schmidt, A. T.; Blaser, H. U. *Org. Process Res. Dev.* **2007**, *11*, 519−523.
(3) Pugin, B.; Blaser, H. U. *Top. Catal.* **2010**, *53*, 953−962.
(4) Ikariya, T.; Murata, K.; Noyori, R. *Org. Biomol. Chem.* **2006**, *4*, 393−406.
(5) Samec, J. S. M.; Bäckvall, J. E.; Andersson, P. G.; Brandt, P. *Chem. Soc. Rev.* **2006**, *35*, 237−248.
(6) Noyori, R.; Ohkuma, T. *Angew. Chem., Int. Ed.* **2001**, *40*, 40−73.
(7) Noyori, R. *Angew. Chem., Int. Ed.* **2002**, *41*, 2008−2022.
(8) Morris, R. H. *Chem. Soc. Rev.* **2009**, *38*, 2282−2291.
(9) Bolm, C.; Legros, J.; Le Paih, J.; Zani, L. *Chem. Rev.* **2004**, *104*, 6217−6254.
(10) Nakazawa, H.; Itazaki, M. *Top. Organomet. Chem.* **2011**, *33*, 27−81.
(11) Junge, K.; Schroder, K.; Beller, M. *Chem. Commun.* **2011**, *47*, 4849−4859.
(12) Enthaler, S.; Junge, K.; Beller, M. *Angew. Chem., Int. Ed.* **2008**, *47*, 3317−3321.
(13) Jothimony, K.; Vancheesan, S.; Kuriacose, J. C. *J. Mol. Catal.* **1985**, *32*, 11−16.
(14) Jothimony, K.; Vancheesan, S. *J. Mol. Catal.* **1989**, *52*, 301−304.
(15) Chen, J. S.; Chen, L. L.; Xing, Y.; Chen, G.; Shen, W. Y.; Dong, Z. R.; Li, Y. Y.; Gao, J. X. *Acta Chim. Sin. (Huaxue Xuebao)* **2004**, *62*, 1745−1750.
(16) Sui-Seng, C.; Freutel, F.; Lough, A. J.; Morris, R. H. *Angew. Chem., Int. Ed.* **2008**, *47*, 940−943.
(17) Sui-Seng, C.; Haque, F. N.; Hadzovic, A.; Pütz, A. M.; Reuss, V.; Meyer, N.; Lough, A. J.; Zimmer-De Iuliis, M.; Morris, R. H. *Inorg. Chem.* **2008**, *48*, 735−743.
(18) Mikhailine, A.; Lough, A. J.; Morris, R. H. *J. Am. Chem. Soc.* **2009**, *131*, 1394−1395.
(19) Sues, P. E.; Lough, A. J.; Morris, R. H. *Organometallics* **2011**, *30*, 4418−4431.
(20) Lagaditis, P. O.; Lough, A. J.; Morris, R. H. *J. Am. Chem. Soc.* **2011**, *133*, 9662−9665.
(21) Meyer, N.; Lough, A. J.; Morris, R. H. *Chem.—Eur. J.* **2009**, *15*, 5605−5610.
(22) Widegren, J. A.; Finke, R. G. *J. Mol. Catal. A: Chem.* **2003**, *198*, 317−341.
(23) Crabtree, R. H. *Chem. Rev.* **2012**, *112*, 1536−1554.
(24) Henrici-Olivé, G.; Olivé, S. *Angew. Chem., Int. Ed.* **1976**, *15*, 136−141.
(25) Tasfy, S. F. H.; Zabidi, N. A. M.; Subbarao, D. *J. Mater. Sci. Eng. A* **2011**, *1*, 9−15.
(26) Schlögl, R. *Angew. Chem., Int. Ed.* **2003**, *42*, 2004−2008.
(27) Phua, P. H.; Lefort, L.; Boogers, J. A. F.; Tristany, M.; de Vries, J. G. *Chem. Commun.* **2009**, 3747−3749.
(28) Rangheard, C.; de Julian Fernandez, C.; Phua, P. H.; Hoorn, J.; Lefort, L.; de Vries, J. G. *Dalton Trans.* **2010**, *39*, 8464−8471.
(29) Stein, M.; Wieland, J.; Steurer, P.; Toelle, F.; Muelhaupt, R.; Breit, B. *Adv. Synth. Catal.* **2011**, *353*, 523−527.
(30) Li, W. Z.; Xie, S. S.; Qian, L. X.; Chang, B. H.; Zou, B. S.; Zhou, W. Y.; Zhao, R. A.; Wang, G. *Science* **1996**, *274*, 1701−1703.
(31) Rizk, S.; Assouar, B. M.; De, P. L.; Alnot, P.; Bougdira, J. *J. Phys. Chem. C* **2009**, *113*, 8718−8723.
(32) Ruemmeli, M. H.; Schaeffel, F.; Kramberger, C.; Gemming, T.; Bachmatiuk, A.; Kalenczuk, R. J.; Rellinghaus, B.; Buechner, B.; Pichler, T. *J. Am. Chem. Soc.* **2007**, *129*, 15772−15773.
(33) Seah, C.-M.; Chai, S.-P.; Ichikawa, S.; Mohamed, A. R. *Carbon* **2012**, *50*, 960−967.
(34) Nguyen, D. D.; Tai, N.-H.; Chen, S.-Y.; Chueh, Y.-L. *Nanoscale* **2012**, *4*, 632−638.
(35) Comba, F. N.; Rubianes, M. D.; Herrasti, P.; Rivas, G. A. *Sens. Actuators, B* **2010**, *B149*, 306−309.
(36) He, C.; Tian, G.; Liu, Z.; Feng, S. *Org. Lett.* **2010**, *12*, 649−651.
(37) Yan, J.-M.; Zhang, X.-B.; Han, S.; Shioyama, H.; Xu, Q. *Angew. Chem., Int. Ed.* **2008**, *47*, 2287−2289.
(38) Ban, Z.; Barnakov, Y. A.; Li, F.; Golub, V. O.; O'Connor, C. J. *J. Mater. Chem.* **2005**, *15*, 4660−4662.
(39) Ranganath, K. V. S.; Kloesges, J.; Schäfer, A. H.; Glorius, F. *Angew. Chem., Int. Ed.* **2010**, *49*, 7786−7789.
(40) Costa, N. J. S.; Kiyohara, P. K.; Monteiro, A. L.; Coppel, Y.; Philippot, K.; Rossi, L. M. *J. Catal.* **2010**, *276*, 382−389.
(41) Prokopchuk, D. E.; Sonnenberg, J. F.; Meyer, N.; Iuliis, M. Z.-D.; Lough, A. J.; Morris, R. H. *Accepted.*
(42) Lin, Y.; Finke, R. G. *Inorg. Chem.* **1994**, *33*, 4891−4910.
(43) Ranganath, K. V. S.; Glorius, F. *Catal. Sci. Technol.* **2011**, *1*, 13−22.
(44) Besson, C.; Finney, E. E.; Finke, R. G. *J. Am. Chem. Soc.* **2005**, *127*, 8179−8184.
(45) Clark, T. J.; Jaska, C. A.; Turak, A.; Lough, A. J.; Lu, Z. H.; Manners, I. *Inorg. Chem.* **2007**, *46*, 7394−7402.
(46) Cho, W. K.; Lee, J. K.; Kang, S. M.; Chi, Y. S.; Lee, H. S.; Choi, I. S. *Chem.—Eur. J.* **2007**, *13*, 6351−6358.
(47) Buil, M. L.; Esteruelas, M. A.; Niembro, S.; Oliván, M.; Orzechowski, L.; Pelayo, C.; Vallribera, A. *Organometallics* **2010**, *29*, 4375−4383.
(48) Mori, K.; Kondo, Y.; Yamashita, H. *Phys. Chem. Chem. Phys.* **2009**, *11*, 8949−8954.
(49) Hu, A.; Yee, G. T.; Lin, W. *J. Am. Chem. Soc.* **2005**, *127*, 12486−12487.
(50) Panella, B.; Vargas, A.; Baiker, A. *J. Catal.* **2009**, *261*, 88−93.
(51) Jansat, S.; Gómez, M.; Philippot, K.; Muller, G.; Guiu, E.; Claver, C.; Castillón, S.; Chaudret, B. *J. Am. Chem. Soc.* **2004**, *126*, 1592−1593.
(52) Alonso, F.; Riente, P.; Yus, M. *Acc. Chem. Res.* **2011**, *44*, 379−391.
(53) Lihl, F. *Z. Metallkd.* **1953**, *44*, 160.
(54) Jaska, C. A.; Temple, K.; Lough, A. J.; Manners, I. *J. Am. Chem. Soc.* **2003**, *125*, 9424−9434.
(55) Bayram, E.; Linehan, J. C.; Fulton, J. L.; Roberts, J. A. S.; Szymczak, N. K.; Smurthwaite, T. D.; Özkar, S.; Balasubramanian, M.; Finke, R. G. *J. Am. Chem. Soc.* **2011**, *133*, 18889−18902.
(56) Lagaditis, P. O.; Lough, A. J.; Morris, R. H. *Inorg. Chem.* **2010**, *49*, 10057−10066.
(57) Hornstein, B. J.; Aiken, J. D.; Finke, R. G. *Inorg. Chem.* **2002**, *41*, 1625−1638.
(58) Tolman, C. A. *Chem. Rev.* **1977**, *77*, 313−348.
(59) Grosvenor, A. P.; Kobe, B. A.; Biesinger, M. C.; McIntyre, N. S. *Surf. Interface Anal.* **2004**, *36*, 1564−1574.
(60) Wagner, C. D.; Naumkin, A. V.; Kraut-Vass, A.; Allison, J. W.; Powell, C. J.; John, R. Rumble, J. In *NIST Standard Reference Database 20*; U.S. Department of Commerce: 2003; Vol. Version 3.5.
(61) Skomski, R. *J. Phys.: Condens. Matter* **2003**, *15*, R841−R896.
(62) Witham, C. A.; Huang, W.; Tsung, C.-K.; Kuhn, J. N.; Somorjai, G. A.; Toste, F. D. *Nat. Chem* **2010**, *2*, 36−41.
(63) Campbell, E. J.; Zhou, H.; Nguyen, S. T. *Org. Lett.* **2001**, *3*, 2391−2393.
(64) Santini, R.; Griffith, M. C.; Qi, M. *Tetrahedron Lett.* **1998**, *39*, 8951−8954.
(65) Banfi, L.; Narisano, E.; Riva, R. In *e-EROS Encyclopedia of Reagents for Organic Synthesis*; Wiley: 2001.
(66) Alfons, B. *J. Mol. Catal. A: Chem.* **1997**, *115*, 473−493.
(67) Demers-Carpentier, V.; Goubert, G.; Masini, F.; Lafleur-Lambert, R.; Dong, Y.; Lavoie, S.; Mahieu, G.; Boukouvalas, J.; Gao, H.; Rasmussen, A. M. H.; Ferrighi, L.; Pan, Y.; Hammer, B.; McBreen, P. H. *Science* **2011**, *334*, 776−780.
(68) Wang, C. M.; Baer, D. R.; Amonette, J. E.; Engelhard, M. H.; Qiang, Y.; Antony, J. *Nanotechnology* **2007**, *18*, 255603.
(69) Bedford, R. B.; Betham, M.; Bruce, D. W.; Davis, S. A.; Frost, R. M.; Hird, M. *Chem. Commun.* **2006**, 1398−1400.
(70) Hoch, L. B.; Mack, E. J.; Hydutsky, B. W.; Hershman, J. M.; Skluzacek, J. M.; Mallouk, T. E. *Environ. Sci. Technol.* **2008**, *42*, 2600−2605.
(71) Kavaliunas, A. V.; Taylor, A.; Rieke, R. D. *Organometallics* **1983**, *2*, 377−383.
(72) Kyriakou, G.; Beaumont, S. K.; Lambert, R. M. *Langmuir* **2011**, *27*, 9687−9695.